RSC Advances

PAPER

View Article Online
View Journal | View Issue

Cite this: *RSC Adv.*, 2016, **6**, 7288

Synthesis, preclinical evaluation and molecular modelling of macrocyclic appended 1-(2-methoxyphenyl)piperazine for 5-HT_{1A} neuroreceptor imaging†

Puja Panwar Hazari,[a] Surbhi Prakash,[ab] Virendra Kumar Meena,[ab] Niraj Singh,[a] Krishna Chuttani,[a] Nidhi Chadha,[a] Pooja Singh,[ab] Shrikant Kukreti[b] and Anil Kumar Mishra*[a]

Received 9th July 2015
Accepted 6th January 2016

DOI: 10.1039/c5ra13432c

www.rsc.org/advances

5-HT_{1A} receptors are known to be implicit in a number of neuropsychiatric fluctuations related to mood and anxiety. Their visualization in the human brain using PET, SPECT or MRI is of great importance in the management and treatment of neurological disorders. The present work focuses on the metal complexes (Gd^{3+}, Eu^{3+} and Ga^{3+}) of DO3A-butyl-MPP to be used as brain (cerebral cortex, hippocampus, and amygdala) imaging agents using different modalities. Synthesis of 2,2′,2″-(10-(2-(4-(4-(2-methoxyphenyl)piperazin-1-yl)butylamino)-2-oxoethyl)-1,4,7,10-tetraazacyclododecane-1,4,7-triyl) triacetic acid (DO3A-butyl-MPP) was achieved by conjugating the chloroacetylated derivative of 1-(2-methoxyphenyl)piperazine-butylamine with trisubstituted cyclen with subsequent cleavage with trifluoroacetic acid (TFA). The resulting compound was then labeled with $GdCl_3$ and $^{68}GaCl_3$ to perform MRI (relaxivity studies) and PET respectively. The longitudinal relaxivity (r_1), and transverse relaxivity (r_2), were determined to be 6.66 and 11.486 mM^{-1} s^{-1} respectively on 7 T at 21 °C. The SD (Sprague Dawley) rat brain uptake was 3.91% ID per g (percentage of the injected dose per gram) at 30 min post injection. Homology modeling and docking studies at the shallow antagonist binding pocket of 5-HT_{1A} show a high *G* score of −12.132 that confers high binding of the ligand at the target receptor.

Introduction

Radiopharmaceuticals that bind to CNS receptors *in vivo* are potentially useful for understanding the pathophysiology of a number of neurological and psychiatric disorders, their diagnosis and treatment.[1] The neurotransmitter serotonin (5-hydroxytryptamine, 5-HT) is involved in various central nervous system functions and psychiatric disorders.[2] The receptors that are activated by 5-HT have been classified into different classes, of which the 5-HT_{1A} receptors have been implicated in the pathogenesis of depression, anxiety, schizophrenia, epilepsy, and eating disorders.[3] For the visualization of these receptors, several ligands have been evaluated, starting from the lead structure of WAY-100635, a potent antagonist whose residue, 1-(2-methoxyphenyl)piperazine (MPP), is known to bind with high affinity to the serotonin receptors.[4] Many ^{11}C and ^{18}F radiolabeled derivatives of WAY-100635 have been synthesized and evaluated for use in positron emission tomography.[5] The radiolabeling of *p*-MPPF with ^{18}F, yielding a fluoro-analogue of WAY-100635 has provided encouraging results *in vivo* by autoradiography in cats, monkeys and human beings.[6]

Despite the success of these tracers as PET imaging agents, the dependency on a nearby cyclotron for radioisotope production and high cost of production has redirected the interest in development of a WAY-100635 analogue incorporating radionuclide that is easily available commercially and has low cost per dose.[7] Moreover, complexes of macrocyclic polydentate ligands based on 1,4,7,10-tetraazacyclododecanetetraacetic acid (DOTA) with radioactive metals are used in potential diagnostic/therapeutic applications.[8] Additionally, DOTA is known to form stable complexes with many metal ions, such as Ga(III), Gd(III), Eu(III), Tb(III) ions.[9] The set of coordinating donor atoms (four nitrogens and four oxygens) wraps around a metal(III) ion in a very efficient way to yield complexes endowed with a very high thermodynamic and kinetic stability.[10]

Thus, in this current study we have designed and synthesized macrocyclic chelating agent covalently linked to 1-(2-

[a]*Division of Cyclotron and Radiopharmaceutical Sciences, Institute of Nuclear Medicine and Allied Sciences, Brig SK Mazumdar Road, Delhi-110054, India. E-mail: akmishra63@gmail.com*

[b]*Department of Chemistry, University of Delhi, Delhi-110007, India*

† Electronic supplementary information (ESI) available: Fig. S1–S25 NMR and mass spectra (ESI and high resolution mass spectra) characterization details of all synthesized compounds, cytotoxicity graph, human serum stability, radioligand binding assays, radio HPLC and radio TLC, molecular modeling studies, calibration curves and specific activity. See DOI: 10.1039/c5ra13432c

methoxyphenyl) piperazine and radiolabeled with ^{68}Ga, which do not require the presence of a nearby cyclotron for its production. ^{68}Ga is a positron emitting isotope which is produced from generator with half-life of 67.71 min. Gallium-based radiopharmaceutical preparation is easy and fast and an alternative to the preparation of ^{18}F- or ^{11}C-labeled PET agents, leading to a minimum loss of activity.[11] The present molecule has also been complexed with Gd(III) to show its properties as a MR contrast agent as MRI provides unmatched and/or unparalleled soft tissue details alongside giving plethora of functional information.

Considering no single modality is perfect and sufficient to gain all the necessary information, the combination of multiple molecular imaging techniques can offer synergistic advantages over any modality alone.[12] Therefore, we have attempted to synthesize a 5-HT$_{1A}$ antagonist which can be utilized for neuroimaging using PET as well as MRI.[13] We hereby report an efficient scalable strategy for the synthesis of 1-(2-methoxyphenyl)piperazine functionalized macrocyclic chelating agent DO3A-butyl-MPP in good yield (80–85%).

The macrocyclic ligand has been designed on the basis of structure–activity relationship (SAR) studies reported in the literature for enhanced affinities towards the target receptors.[14] In order to achieve optimal selectivity and affinity the macrocyclic ligand was constructed keeping in consideration the following aspects; firstly methoxyphenylpiperazine moiety has basic nitrogen which can be functionalized easily. Secondly, functionalization with butyl linker increases affinity towards the 5-HT$_{1A}$ receptor. Attaching methoxyphenylpiperazine moiety to macrocycle ligand provides an excellent agent for imaging purpose. It is well documented in literature[4h] that $(CH_2)_n$ is a spacer attached to –NH of the arylpiperazine, with respect to n two to four methylene groups appear optimal. This chain length (n) can influence affinity and selectivity of the molecule.[15] It is known from the previous reports, that the linker length significantly enhances the binding affinity towards 5-HT$_{1A}$ receptors and reduce the affinity for α_1-adrenergic as well. The most optimal condition for high binding affinity is provided by linker length of $(CH_2)_n$, $n = 4$ with subnanomolar K_i value for 5-HT$_{1A}$ receptor ligands.[16] When there is a change in value of 'n' [*i.e.* $n = 2, 3, 5, 6$] it subsequently reduces the affinity of ligands and disrupts the most optimal condition for high binding to the 5-HT$_{1A}$ receptor. The alkyl amide bond further enhances the affinity by interacting with the receptor, which is suggestive of its hydrophobic nature of interaction.[16]

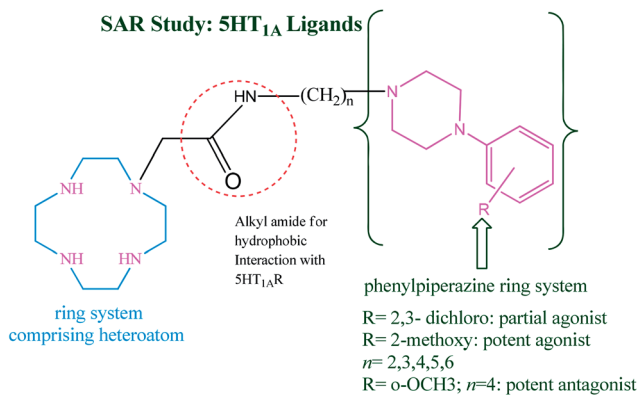

The binding affinity of 5-HT$_{1A}$ receptor ligands towards the aryl substituent group (R = *o*-CH$_3$, *o*-OBu, *o*-OCH$_3$, *o*-NHCOPr, *m*-NHCOPr, *o*-CN, *o*-COOPr, *m*-NH$_2$, *m*-Br) were also evaluated and reported by various groups, suggesting that the *o*-OCH$_3$ group have the highest binding affinity to the 5-HT$_{1A}$ receptors.[17] Moreover, PET radioligands for 5-HT$_{1A}$ with *o*-OCH$_3$ group have been used extensively to track the 5-HT$_{1A}$ neuroreceptor fluctuations in the brain.

We hereby present an efficient approach in the design and synthesis of a multi-functional chelating agent based on 1-(2-methoxyphenyl) piperazine for targeting 5-HT$_{1A}$ receptors in brain.

Results and discussion

Chemistry

1-(2-Methoxyphenyl)piperazine was alkylated with *N*-(4-bromobutyl)phthalimide and cleaved with hydrazine hydrate to give 4-(4-(2-methoxyphenyl)piperazine-1-yl)butan-1-amine (**2**).[18] *N*-(4-Bromobutyl)phthalimide was used to increase the yield of compound (**2**). Compound (**2**) was then chloroacetylated in dichloromethane : water (1 : 1) to yield 2-chloro-*N*-(4-(4-(2-methoxyphenyl)piperazin-1-yl)butyl)acetamide (**3**). Chloroacetylated butyl-MPP (**3**) was conjugated to trisubstituted cyclen (**4**) to give *tert*-butyl-2,2′,2″-(10-(2-(4-(4-(2-methoxyphenyl)piperazin-1-yl)butylamino)-2-oxoethyl)-1,4,7,10-tetraazacyclododecane-1,4,7-triyl)triacetate (**5**) which was further reacted with trifluoroacetic acid (TFA) to cleave the boc groups and obtain the final compound 2,2′,2″-(10-(2-(4-(4-(2-methoxyphenyl) piperazin-1-yl)butylamino)-2-oxoethyl)-1,4,7,10-tetraazacyclododecane-1,4,7-triyl) triacetic acid (**6**) with overall yield of 80–85% starting from 1-(2-methoxyphenyl)piperazine (Scheme 1).

Conjugation of butyl-methoxyphenylpiperazine moiety to macrocycle ligand provides an excellent agent for the complexation of trivalent metal ion for imaging application. The introduction of the bifunctional butyl spacer and conjugation of the DOTA group with MPP accomplished the synthetic design aiming to ensure simplistic and scalable approach with high yield. This was achieved using *N*-(4-bromobutyl)phthalimide which gave the product 4-(4-(2-methoxyphenyl)piperazin-1-yl)butan-1-amine in more than 70% yield after subsequent cleavage of phthalimide group whereas using unprotected bromobutylamine, less than 40% yield was obtained. Direct functionalization of –NH group of methoxyphenylpiperazine with DOTA gave product with less than 20% yield.

For the development of PET imaging agent, DO3A-butyl-MPP was complexed with ^{68}Gallium. Gallium-based radiopharmaceutical preparation is easy and fast, contrary to the preparation of covalently ^{18}F- or ^{11}C-labeled PET agents, leading to a minimum loss of activity. The most important requirements for a Ga(III)-based radiopharmaceutical agent are thermodynamic stability and kinetic inertness during the period of clinical use in order to avoid ligand exchange with the blood serum proteins, such as transferrin. DOTA is also advantageous considering that it can more than saturate Gallium's common

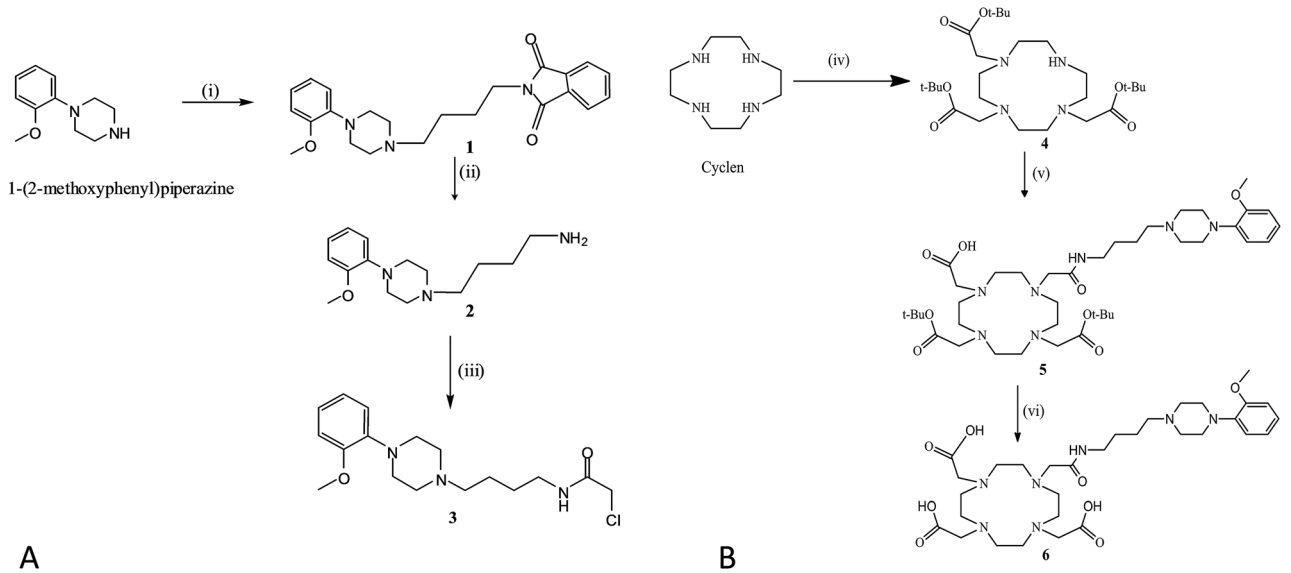

Scheme 1 (a) Synthesis of 2-chloro-*N*-(4-(4-(2-methoxyphenyl)piperazin-1-yl)butyl)acetamide (**3**). Reagents and conditions: (i) ACN, K_2CO_3, 4-bromobutylphthalimide, 70 °C (ii) hydrazine hydrate, ethanol, reflux, 2 h (iii) $ClCH_2COCl$, DCM/H_2O, 0 °C. (b) Synthesis of 2,2′,2″-(10-(2-(4-(4-(2-methoxyphenyl)piperazin-1-yl)butylamino)-2-oxoethyl)-1,4,7,10-tetraazacyclododecane-1,4,7-triyl)triacetic acid (**6**). Reagents and conditions: (iv) ACN, $NaHCO_3$, 0 °C, *tert*-butylbromoacetate (v) ACN, **3**, 70 °C (vi) 20% TFA in DCM, 0 °C.

six coordination sphere, offering free carboxymethyl arms for conjugation to targeting molecules. On achieving encouraging results from PET studies, we extended our approach of developing multifunctional contrast agent towards the prospect of utilization of the ligand DO3A-butyl-MPP as magnetic resonance imaging agent. The coordination chemistry of lanthanide complexes of polyaminocarboxylates is very important because of their application in biomedical sciences as MR contrast agent. It is well known that gadolinium complexes are T_1-weighted MRI contrast agents, and thus the T_1 relaxivity rate is an important parameter. With the aim to synthesize MR imaging agent possessing potential of targeting brain region, DO3A-butyl-MPP was complexed with gadolinium and its relaxation properties were investigated. To assess the hydration state of complex, the luminescence lifetime measurements on Eu(III) complex of DO3A-butyl-MPP were conducted.

Relaxometric studies

The enhancement of the longitudinal relaxation rate of water protons ($1/T_1$) occurs due to the presence of paramagnetic Gd(III) in complexes. The proficiency of the Gd(III) complexes is expressed in terms of relaxivity (r_1, $mM^{-1}\ s^{-1}$) values, which is the increase in the longitudinal proton relaxation rates induced by 1 mM. Longitudinal and transverse proton spin relaxation rates were measured for Gd complex of DO3A-butyl-MPP in an aqueous solution (pH-7) at various concentrations (0.625, 1.25, 2.5, 5, 10, 20, 40, 80 mM). A contrast enhancement in T_1-weighted images in the concentration range of 0.625-20 mM of Gd-DO3A-butyl-MPP exhibited in MR studies (Fig. 1A), the effect being more marked at lower concentrations. At concentration as low as 0.625 mM, enhanced contrast was obtained whereas darker image intensity was observed at higher concentration of the complex. At low concentration, an increase in contrast results to an increase in signal intensity due to effect on T_1 concentration of the Gd(III) complex.

A plot of relaxivities as a function of the concentration of this complex was plotted (Fig. 1B and C) where the values of r_1 and r_2 were calculated from the slope of $1/T$ values obtained from samples at different concentrations. The measured relaxivities arise from the exchange between the coordinated water molecules and the surrounding water molecules in solution. The

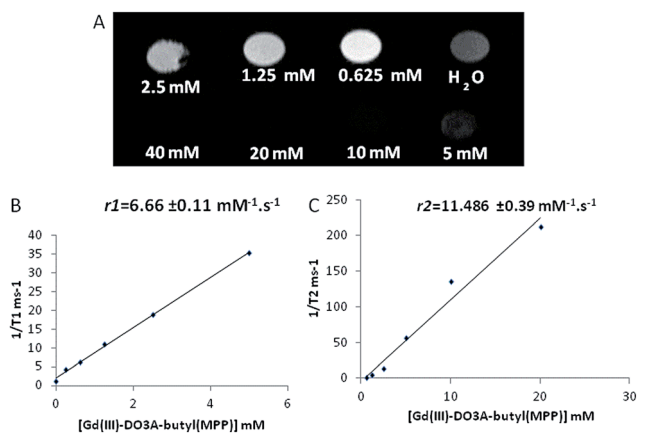

Fig. 1 (A) T_1 weighted image of Gd-DO3A-butyl-MPP at different concentrations varying from 0.625 mM to 40 mM. Concentration range of 0.625–40 mM of Gd-DO3A-butyl-MPP exhibited in MR studies, the effect being more marked at lower concentrations. At concentration as low as 0.625 mM, enhanced contrast was obtained whereas darker image intensity was observed at higher concentration of the complex. (B & C) *In vitro* MR measurement of the longitudinal and transverse relaxivity, r_1 and r_2 of Gd-DO3A-butyl-MPP with varying concentrations.

longitudinal relaxivity r_1, and transverse relaxivity r_2, was determined to be 6.66 ± 0.11 mM^{-1} s^{-1} and 11.49 ± 0.39 mM^{-1} s^{-1} respectively. Thus the r_1 value and stability constant with the M(III) metal ion promises its potential as an MR contrast agent for various *ex vivo* imaging purposes of 5-HT_{1A} neuroreceptor in brain.

Assessment of number of coordinated water molecules (q)

Assessment of the number of coordinated water molecules (q) was carried out using luminescence lifetime measurements. The values of luminescence lifetimes calculated for Eu-DO3A-butyl-MPP in H_2O and D_2O are depicted in Table 1. The hydration number "q" calculated from equation of Supkowski and Horricks comes out to be 1.43. It indicates that more than one water molecule is bound in inner sphere.

The lifetime increases substantially in D_2O solution due to the known sensitivity of Eu(III) luminescence towards deuterated solvent. Since Eu(III) neighbour Gd(III) in the periodic table and has similar ionic radii, the results of luminescence technique gives a good estimate for the hydration number of the corresponding Gd(III) chelate. Thus the hydration number "q" indicated that more than one water molecule probably bound to the inner sphere of Gd(III). Attempts have been made to increase the low hydration number of Gd(III) chelates but the toxicity concerns of the Gd(III) chelates hamper this way of increasing the proton relaxivity. The thermodynamic and kinetic stabilities of the complex decreases considerably when more than one coordination site is occupied by water.[19] However as seen through potentiometric titrations, the ligand is found to form stable complex with Gd(III) which eliminates this risk of toxicity.

Determination of protonation and stability constant

The protonation constants of DO3A-butyl-MPP and stability constant of the complex was calculated by pH potentiometric titrations. Solutions of Gd(III), Eu(III), Zn(II) and Cu(II) in MilliQ water were prepared by dissolving the appropriate amounts of their salts. For titrations of complexes, an appropriate volume of the previously prepared metal solution was added *via* micropipette to reach the 1 : 1 ligand to metal ratio. The protonation constants of ligand DO3A-butyl-MPP in comparison with DOTA and DTPA are given in Table 2.

The pK_{a1} and pK_{a2} of DO3A-butyl-MPP was found to be lower than DOTA and DTPA indicating better ionization and dissociation at any given pH. pK_{a3} was found to be comparable for all the chelating systems.

For the determination of kinetic stabilities of the complexes, the rates of exchange (trans-metallation) reactions taking place between the Gd^{3+} complexes and the metal ions Cu^{2+}, Zn^{2+} or Eu^{3+} were studied (Table 3).

The determination of the protonation constants of the ligand and the properties of its metal complexes are useful for determining stable rigid complexes with M(III) metal ions. Since the ligand, DO3A-butyl-MPP is tridentate as compared to DOTA and DTPA the effect of protonation could be seen by lower values of pK_{a1} and pK_{a2}. The stability constant of DO3A-butyl-MPP was slightly lower than DOTA and DTPA but good enough for high binding with M(III) complexes. The amide bond of DO3A-butyl-MPP participates in slightly weaker coordination with Gd^{3+} which lowers the stability constant as compared to DOTA and DTPA.[19] Even though there is reduced affinity of DO3A-butyl-MPP towards Gd^{3+} when compared to DOTA and DTPA, DO3A-butyl-MPP also have lesser tendency to bind with endogenous Ca^{2+}, Zn^{2+} and Cu^{2+} increasing the binding selectivity of DO3A-butyl-MPP for Gd^{3+} over Zn^{2+} and Cu^{2+}. A sufficiently high thermodynamic stability of the Gd(III) complex and good selectivity of the chelating ligand for Gd(III) over other endogenous metal ions such as Cu^{2+}, Zn^{2+} are needed as prior condition for all biomedical applications.

Stability constant of DO3A-butyl-MPP complexes with Eu(III) and Gd(III) showed similar log β. The lower log β values for Cu^{2+} and Zn^{2+} confirmed that DO3A-butyl-MPP forms more stable complex with lanthanide ions, thus it will not undergo trans-metallation with endogenous metal ions.

^{68}Ga radio-complexation of DO3A-butyl-MPP, serum stability and log *P*

The preparation of ^{68}Ga-DO3A-butyl-MPP was simple and efficient by using sodium acetate. The radio-TLC was performed on silica RP18 F256S plate with sodium citrate (0.15 M) as the mobile phase. Radio TLC showed peak at 5.73 for free ^{68}Ga-acetate (<2%) and 3.21 for ^{68}Ga-DO3A-butyl-MPP.

Radiochemical yield was calculated from decay-corrected ^{68}Ga at the end of synthesis (EOS) including SPE purification (Fig. S19 ESI†). The decay corrected radiochemical yield was found to be 86.42 ± 3.9%, n = 40 runs with specific activity of 529.08 GBq μmol^{-1} (decay corrected and SPE purification for 15 min, EOS). After tc18 cartridge purification of ^{68}Ga-DO3A-butyl-MPP, it showed no evidence of presence of free ^{68}Ga. Radio HPLC analysis of the purified product ^{68}Ga-DO3A-butyl-MPP showed 99% radiochemical purity and the presence of only one peak (R_T = 7.8 min) confirms the formation of only one species of the complex which quantitatively reflected the radiochemical purity of the sample

Table 1 Luminescence lifetime measurements of Eu-DO3A-butyl-MPP

Complex	$1/\tau_{H_2O}$ (μs)	$1/\tau_{D_2O}$ (μs)	q
Eu-DO3A-butyl-MPP	2.617	1.257	1.43

Table 2 pK_a values of ligand DOTA, DTPA and DO3A-butyl-MPP

pK_a	DOTA	DTPA	DO3A-butyl-MPP
pK_{a1}	11.14	10.49	9.58
pK_{a2}	9.69	8.37	7.13
pK_{a3}	4.85	4.09	4.78

Table 3 Stability constant of metal complexes of DO3A-butyl-MPP with Gd^{3+}, Zn^{2+}, Eu^{3+}, Cu^{2+}

	Gd-DO3A-butyl-MPP	Eu-DO3A-butyl-MPP	Zn-DO3A-butyl-MPP	Cu-DO3A-butyl-MPP
log β	17.6969	17.4256	7.0897	6.0173

(Fig. S20, ESI†). The optimisation of radiolabeling with respect to pH, temperature, duration of heating and the amount of precursor used in labeling is described in detail in ESI (Fig. S21 ESI†).

The rate of decomplexation of the radiolabeled complex was studied in human serum under physiological conditions at different time intervals of 5, 10, 15, 30, 60, 120 and 180 min. No measurable loss of metal ion from the macrocyclic core and high stability of the radiolabeled DO3A-butyl-MPP were observed (see Fig. S22 ESI†). Thus high specific activity, stability was achieved and log *P* was found to be 2.59. The log *P* of the radiolabeled DO3A-butyl-MPP was found to be lipophilic in nature, appropriate to cross the blood brain barrier.

Cell viability studies of DO3A-butyl-MPP

The *in vitro* cytotoxicity of the ligand, DO3A-butyl-MPP was studied by incubating human embryonic kidney (HEK) cells with varying concentrations of the compound at time intervals of 24, 48 and 72 h. Using 100 μL of HBSS (Hank Balance Saline Solution) as control, experiment was conducted. Significant percentage of viable cells were obtained when HEK cells were treated with low concentrations (1–100 μM) of the compound. After 24 and 48 h incubation of 10 mM concentration of the compound cell survival (percentage relative to untreated controls) in the range of 70–75% was observed (Fig. S23, ESI†). The cytotoxicity studies assessed in normal HEK cells showed high IC_{50} indicating its safe and favorable applications to be used in nuclear medicine imaging techniques.

Radioligand binding assay

The specificity of the 1-(2-methoxyphenyl)piperazine functionalized compound to bind to the cell surface receptors on primary hippocampal culture cells was examined by radioligand receptor binding assays using ^{68}Ga-DO3A-butyl-MPP as the labeled ligand. Primary hippocampal cells were cultured as reported in literature.[20] It has been demonstrated previously that moderate to heavy signal were detected for 5-HT_{1A} mRNA transcripts in hippocampal neurons and glial cells.[21] The specificity of the 1-(2-methoxyphenyl)piperazine functionalized compound to bind to the cell surface receptors on primary hippocampal culture cells was examined by radioligand receptor binding assays using ^{68}Ga-DO3A-butyl-MPP as the labeled ligand.

Non-specific binding was obtained by using 100-fold excess of unlabeled serotonin and WAY-100635. Analysis of the binding curve exhibited saturable binding of the radioconjugate in subnanomolar range. Scatchard plot analysis revealed that the labeled compound exhibited high affinity on hippocampal neuronal cultures with a K_d value of 0.64 nM and 0.27 nM in competitive binding assay with serotonin and WAY-1000635 respectively.

The binding affinity of the compound, DO3A-butyl-MPP on the targeted receptors was determined by harvesting different parts of brain expressing serotonin receptors and transporters. 5-HT_{1A} receptor binding assay exhibited lower affinity of ^{68}Ga-DO3A-butyl-MPP towards 5-HT_{2A} receptors (K_d = 136 ± 3.4) than 5-HT_{1A} receptors (K_d = 0.39 ± 0.08) in brain homogenates (Table 4). Scatchard plot of the radioligand binding assays of 5-HT_{1A}, 5HTT and 5-HT_{2A} brain homogenate are given in ESI† (Fig. S24).

A subnanomolar affinity for the 5-HT_{1A} receptor was obtained for the above derivative in the *in vitro* binding assay which was sufficiently high to carry out imaging. The selectivity of the complex for 5-HT_{1A} receptors was observed to be 1000 times as high as for 5-HT_{2A} receptors (Table 4). 5-HTT also showed high affinity with a value of 56 ± 0.7 nM.

PET image of rat whole brain

The results found in the micro PET imaging of SD (Sprague Dawley) rat brain indicated that the radiotracer showed remarkable accumulation in the rat brain striatum over 30 min compared with surrounding normal tissue (Fig. 2). The decline in activity was observed after 30 min. This could be well supported by the fact that terminal elimination half life of antagonist WAY 100635 is also fast with a value of 33 min.[22]

The radioactivity distribution was in concordance with the known 5-HT_{1A} receptor distribution, with high uptake of radioactivity in hippocampus, caudate putamen and amygdala (Fig. 2A). The time activity curves revealed accumulation of the radioligand in whole brain over the first few minutes which were followed by a clearance of the compound from hippocampus (Fig. 2).

The pre-treatment experiment with WAY-100635 (known 5-HT_{1A} antagonist) markedly reduced the level of radioactivity in all examined regions. Cerebellum was used as a reference region for the calculation of binding potential due to the low 5-HT_{1A} receptor density. Rat MRI atlas was superimposed on the micro PET for anatomical confirmation of the brain regions. VOI analysis was done using PMOD, data is determined as VOI (CPS cm^{-3}) brain region/VOI (CPS cm^{-3}) cerebellum. VOI analysis showed highest uptake in hippocampus followed by hippocampus and amygdala (Fig. 3). VOI of 5.606 in hippocampus region and 2.59 in caudate putamen was observed. VOI of 3.2 and 2.48 were in amygdala and

Table 4 Dissociation constants of DO3A-butyl-MPP for 5-HT_{1A}, 5-HT_{2A}, and 5-HTT receptors[a]

K_d (nM)	5-HT_{1A}	5-HT_{2A}	5-HTT
^{68}Ga-DO3A-butyl-MPP	0.39 ± 0.09	136 ± 3.4	56 ± 0.7

[a] Nonspecific binding was determined by serotonin, ketanserin and paroxetine.

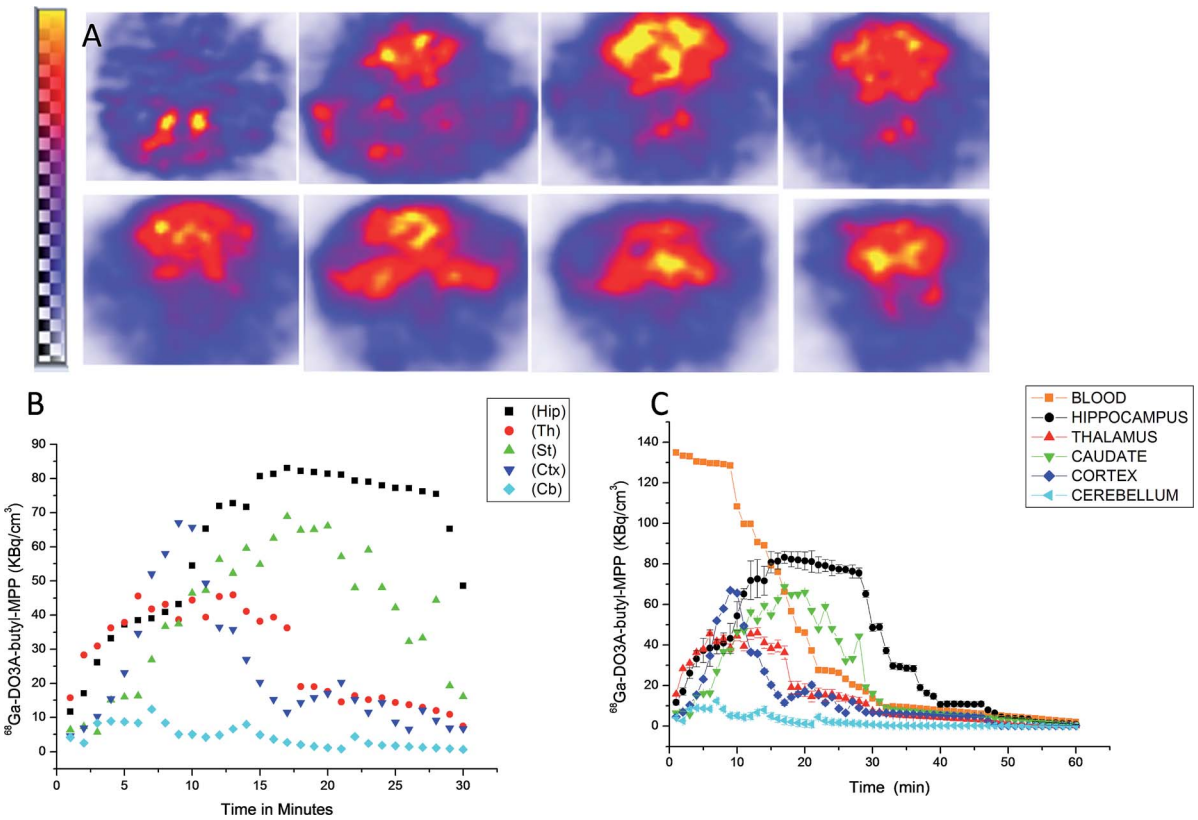

Fig. 2 (A) 0–30 minutes summation images of rat brain coronal microPET scan depicting activity in different section (slices) of the brain. (B) Time activity curve (TAC) of different regions for 30 minutes and (C) TAC for 60 minutes post ^{68}Ga-DO3A-butyl-MPP injection in rat ($n = 5$).

hypothalamus respectively as compared to the cerebellum with a VOI of 1.1.

Regional uptake in rat brain

Regional binding indices were calculated by % ID per g of the different regions of the brain by their respective weights (Fig. 4). In regional biodistribution experiments, the hippocampus showed the highest uptake of radiolabeled compound, followed by the caudate putamen which showed a binding of 1.499% ID per g and cerebellum showed least uptake with a value of 0.08% ID per g. Whole brain uptake at 30 min increased to 3.724% ID per g and 73% fall of activity at 60 min. The values were concordant with the VOI obtained in PET brain scan. The 5-HT receptor-rich regions showed significantly higher binding index than the cerebellum.

Plasma clearance and biodistribution

The plasma clearance and *in vivo* biodistribution of ^{68}Ga-DO3A-butyl-MPP was studied in SD rats at different time intervals.

Plasma clearance indicates the clearance rate from the body. The biological half life $t_{1/2}$ (fast) results in the increase in target to non target ratio. Biodistribution studies were performed to study the accumulation pattern of tracer in the whole body. It was observed that the clearance of complex was through the renal and hepatobiliary routes.

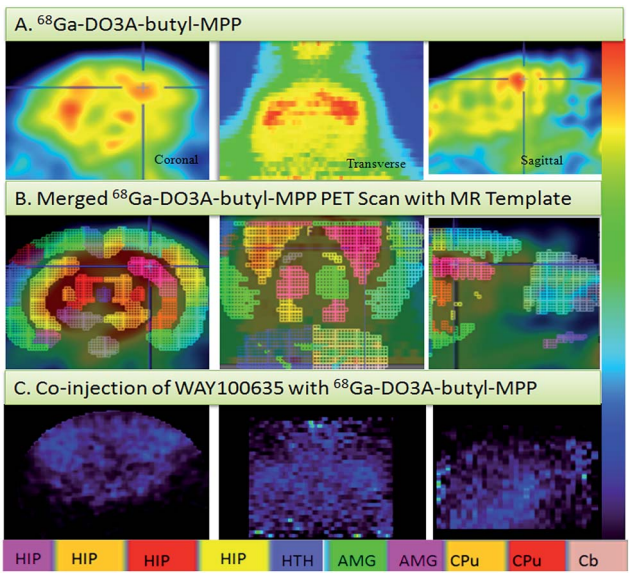

Fig. 3 MicroPET images of rat brain showing coronal, transverse and sagittal sections respectively after the intravenous injection of 37 MBq of ^{68}Ga-DO3A-butyl-MPP. (A) SD rat depicting high accumulation of radioactivity in hippocampus, amygdala and caudate putamen. (B) Coregisteration of rat MRI atlas on the microPET scan for anatomical confirmation of the brain regions was done using PMOD and (C) Blocking studies with WAY-100635.

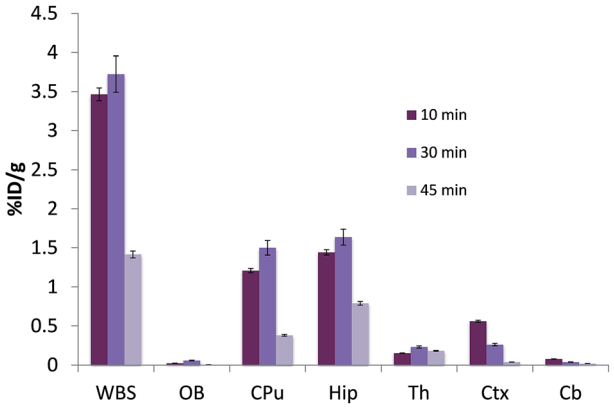

Fig. 4 Regional distribution of ^{68}Ga-DO3A-butyl-MPP in SD rat brain. WBS = whole brain section Hip = hippocampus, Th = thalamus, Ctx = frontal and parietal cortex, CPu = caudate putamen, Cb = cerebellum at 10, 30 and 45 min post injection.

The plasma clearance followed a biphasic trend with a rapidly clearing initial phase followed by slow phase. Plasma clearance rate (C_R) was found to be 37.39 ± 0.31 μg mL^{-1} min^{-1} (Fig. 5).

In biodistribution studies, major accumulation of the labeled compound was observed in kidneys (14.62 ± 0.52% ID per g) followed by liver (6.19 ± 0.61% ID per g) at 2 h showing that the complex is excreted by renal and hepatobiliary routes. Retention of radioactivity in the non-target organs (lungs, spleen, intestine *etc.*) was less than 2.0% ID per g at 4 h post injection. Accumulation in lungs attributed to the lipophilic nature of complex. The retention of activity follows a declining trend in the all the organs for the later time points except for the kidneys at 4 h, wherein the clearance was observed at 8-10 h.

In vivo biodistribution of ^{68}Ga-DO3A-butyl-MPP in SD rats showed 3.52 ± 0.39% ID per g activity in brain at 10 min and 3.91 ± 0.54% ID per g activity at 30 min which drastically decreased at 2 h with a value of 0.48 ± 0.03% ID per g activity. The selective high brain uptake could be seen in regional biodistribution studies which were found concomitant with the VOIs generated from the PET studies. Cardiac uptake was seen at early time points (Fig. 6).

MR imaging

The preliminary *in vivo* imaging was done on rat brain with and without injection of the Gd(III)-complex, which shows that the ligand Gd-DO3A-butyl-MPP at 2 mM was showing enhanced images as compared to the control brains. T_1-weighted signal enhancement was observed on an *in vivo* MRI, notably within hippocampus, which further supports the specificity of the complexed ligand towards 5-HT$_{1A}$ receptors.

The T_1 were statistically decreased by Gd-DO3A-butyl-MPP at 2 mM administration (0.176 mmol kg^{-1}) for hippocampus compared to baseline scan (Fig. 7A). The enhancement of *in vivo* MRI in the control brains was statistically significant with a positive signal at 7 T. It is worthwhile to note that the shortening of T_1 relaxation was observed in treated rats at 30 min post injection at a concentration of 0.176 mmol kg^{-1} of Gd-DO3A-butyl-MPP, as compared to control rats. There was increase in T_1 relaxation on different regions of brain when WAY100635 (0.2 mmol kg^{-1}) and Gd-DO3A-butyl-MPP (0.176 mmol kg^{-1}) were co administered at 30 min pi (Fig. 7B).

It was also observed that the cerebral blood flow was increased when the Gd(III)-DO3A-buyl-MPP was given alone which is an indication of antagonistic property of the compound. It can be hypothesized from the study conducted on rats that in pathological state when there is an up regulation of 5-HT$_{1A}$ receptors, this contrast agent could be useful in visualizing the uptake at high density and high concentration. It could be useful as a surrogate tracer of ^{68}Ga-DO3A-buyl-MPP for MR imaging.

Theoretical evidence

Molecular modeling and docking studies with monomeric 5-HT$_{1A}$ receptor models. Homology modeling and flexible docking studies has been performed for DO3A-butyl-MPP with human 5-HT$_{1A}$ homology modeled receptor. The 5-HT$_{1A}$ model was optimized; refined and Ramachandran plot validates the models where residues are present in allowed region without any steric clashes (Fig. 8A). The reliable modeling of TM region

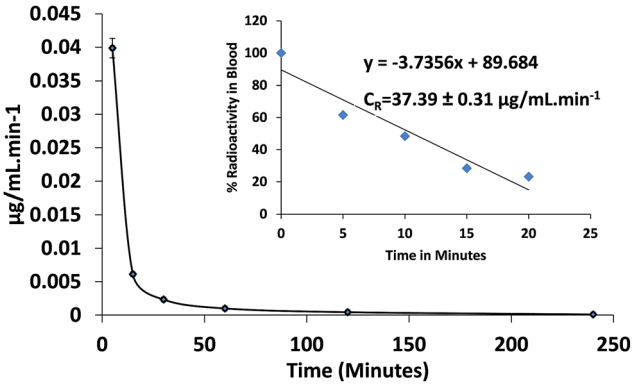

Fig. 5 Plasma clearance of ^{68}Ga-DO3A-butyl-MPP (inset: initial clearance up to 20 min).

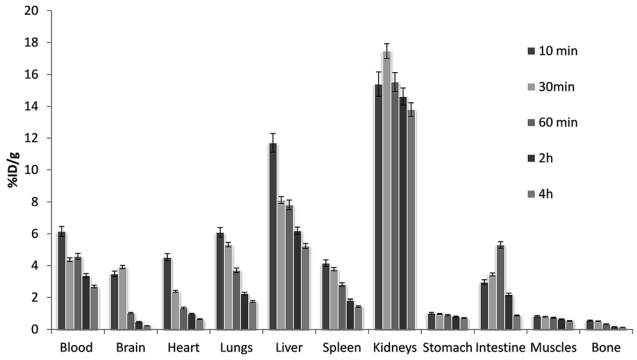

Fig. 6 Biodistribution of ^{68}Ga-DO3A-butyl-MPP in SD rats following intravenous injection of 8.14 MBq activity.

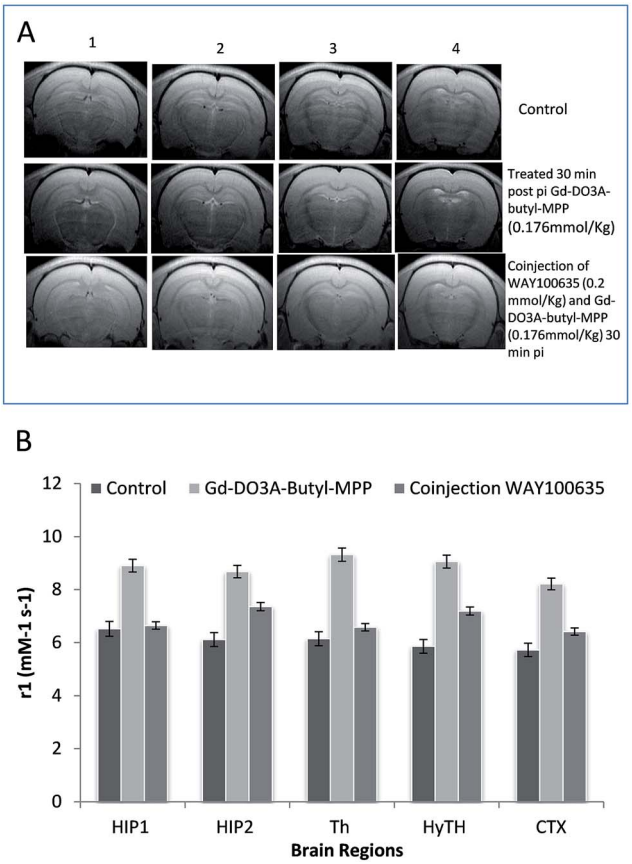

Fig. 7 (A) *In vivo* MR imaging in control and treated SD rats depicting T_1 shortening in 30 min images post Gd-DO3A-butyl-MPP (0.176 mmol kg^{-1}) injection. (B) Representation of relaxivity with respect to the different regions in the brain.

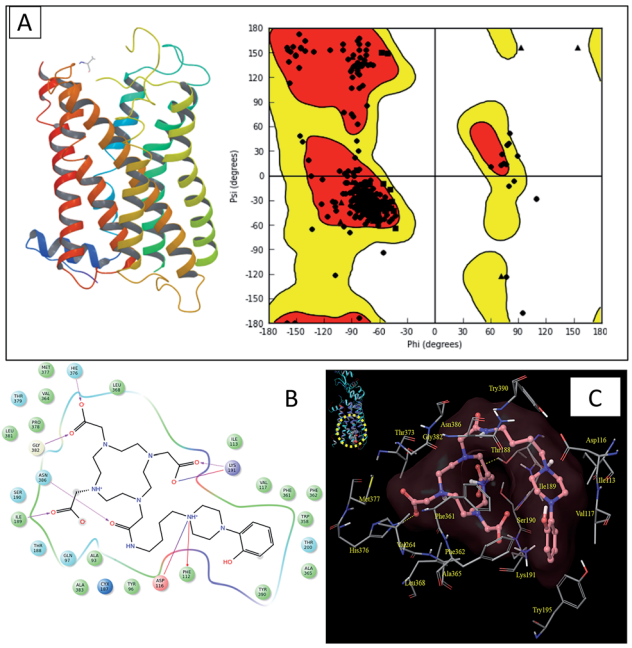

Fig. 8 (A) Model of the human 5-HT_{1A} receptor and Ramachandran plot showing the transmembrane helices in different colours. (B) Two dimensional view of DO3A-butyl-MPP with 5-HT_{1A} receptor where green colored are hydrophobic, light blue are polar, red are negative and purple are positive charged residues. Pink lines are hydrogen bonds, red lines are π–cation interactions. (C) Three dimensional view of DO3A-butyl-MPP (pink carbon layout) at the binding pocket of 5-HT_{1A} homology modeled receptor. Yellow dashed lines are showing the hydrogen bonds.

is important since ligand binding pockets lies in TM region of the 5-HT_{1A} monomer (Fig. 8A).

Three antagonist; *p*-MPPF, BMMP and WAY-100635 were used in the docking studies to understand the binding pose of our ligand with 5-HT_{1A} receptor.[23]

Our molecular modelling results showed a promising results for thermodynamic parameters obtained by docking of the DO3A-butyl-MPP and interactive residue present in the active site of the 5-HT_{1A} receptor. DO3A-butyl-MPP was aligned in hydrophobic pocket conserved in all three studied antagonists, *p*-MPPF, BMMP and WAY-100635, the Glide XP scoring mode in flexible docking has predicted the minimized energy complexes in terms of XP score (Table 5). The antagonist *p*-MPPF is involved in π–π interactions with Phe362 and hydrogen bonding with backbone of Ile189 whereas MefWAY is involved in π–π interactions Arg181 and hydrogen bonding with backbone of Ile189. But in case of WAY-100635, one additional π–π interactions with Phe361 was obtained (see Fig. S25 ESI†).

The docking pose of DO3A-butyl-MPP at the shallow antagonist binding pocket of 5-HT_{1A} was found to have high *G* score of −12.132.

The high *G* score signifies the contribution due to important hydrophobic residues surrounding the ligands. In the ligand, DO3A-butyl-MPP, the carboxylate groups and carbonyl moiety of DOTA is involved in hydrogen bonding with side chain residues, His376, Gly382, Ile189 and Lys191. In addition, π–cation interactions were observed for protonated –NH of piperazine moiety with Phe112. This interaction is an example of non covalent bonding between a monopole (cation) and a quadrupole (π system). Here, the cation is nitrogen which is protonated and π-electrons are in residue Phe112.

In addition to the above interactions, the aromatic ring of piperazine moiety of DO3A-butyl-MPP was involved in π–π stacking with Phe361, Phe362 and hydrogen bond interactions with the side chain of Asp116. The resident binding pocket of both uncomplexed and complexed DO3A-butyl-MPP was found to be conserved and comparable to our pervious results[24] with known antagonists in which docking was performed in flexible mode showing appreciable *G*-score.

The Asp116 interactions with azapirones, buspirone and sunepitron are well known with piperazine amine[25] as in case of DO3A-butyl-MPP. This binding mode is in general agreement with putative binding modes suggested in a published ligand-supported homology model of 5-HT_{1A} receptor.[26] Also the binding pose is quite consistent with the available experimental studies[25] and importance of these residues is evidenced by site-directed mutagenesis. From docking pose, the antagonist binding pocket was found to be relatively shallow and involved in various interactions at the site.

Table 5 IFD Glide score and ligand interactions of antagonists MefWAY, WAY-100635 and *p*-MPPF and DO3A-butylMPP

	Residual interactions		*G* score monomeric
Ligand	Non-polar residues	Polar residues	IFD
DO3A-butyl-MPP	Ile189, Asp116, Phe112, Phe362, Gly382	Lys191, Thr200, Asn386	−12.132
p-MPPF	Val117, Cys120, Ile189, la203, Phe361, Phe362, Val364, Ala365, Leu368	Lys191, Thr200	−9.11
MefWAY	Ile189, Phe361, Leu368, Gly382, Arg181	Thr196, Ser190, Lys191, Ser199, Thr379	−9.81
WAY-100635	Ile189, Tyr195, Phe361, Leu368, Gly382	Thr196, Thr200, Ser190, Lys191, Ser199, Thr379	−8.81

Although promising, PET compounds, particularly ^{11}C compounds, are generally limited to those facilities with a cyclotron and the high cost hinders commercialization of viable agents which is driving the need to develop ^{68}Ga-based agents that can target 5-HT_{1A}. Progress in receptor pharmacology with PET radiotracers has led to the design of numerous candidate for CNS imaging. Fragments of WAY100635, (*i.e.* arylpiperazine), have been combined with various bifunctional chelates consisting of a ligand that binds to technetium-99m and a linker that joins to the targeting vector. Johannsen *et al.* prepared a WAY-based complex using an N_2S_2 chelate to bind to ^{99m}Tc including similar derivatives of arylpiperazine linked to other technetium(v) chelates (N_xS_y or N_xP_y, $x = 1$–4, $y = 4 - x$).[27] Although their IC_{50} and K_i values appear promising, these agents have low or negligible brain uptake. To date, no ^{68}Ga labeled compound has been developed which can image the 5-HT_{1A} receptor *in vivo*. DO3A-butyl-MPP provides efficient macrocyclic framework for complexation of M^{3+} metal ions for multiple biomedical applications. Its improved affinity and selectivity with high brain uptake is evident through PET imaging in rat brain which could plausibly be translated clinically.

Conclusions

We have efficiently synthesized a chelating system containing 1-(2-methoxyphenyl)piperazine unit as a vector for evaluation of 5-HT_{1A} receptors. Keeping in mind the concept of multiple imaging modalities, the compound has been labeled with Gd(III), Eu(III), and ^{68}Ga so that it can be exploited as MRI and PET imaging agent. Encouraging results have been obtained with all three modalities. The compound (Gd-DO3A-butyl-MPP) has shown longitudinal relaxivity, r_1 of 6.66 mM^{-1} s^{-1} and transverse relaxivity, r_2 of 11.49 mM^{-1} s^{-1} on 500 MHz at 21 °C. Hydration number, '*q*' was found to be 1.43 from luminescence lifetime studies. Compound (^{68}Ga-DO3A-butyl-MPP) shows high affinity for hippocampal cells found in brain, proving its relevance as a CNS imaging system, shown also by the appreciable uptake of radiolabeled compound in brain in PET images. The desired molecule also shows antidepressant actions in the behavioral tests conducted on CMS model of rats, and completely reverses the depression levels. The action of the DO3A-butyl-MPP can be speculated by acting on 5-HT_{1A} *via* SSRI effect, which further supports its potency in treating depression. So the preliminary results and preclinical evaluations of the given compound DO3A-butyl-MPP show it as a favorable molecule and promises good potential as a CNS imaging system which can be used as a MR contrast, and PET imaging system. This will also encourage the development of brain imaging compounds for different applications.

Experimental

General

1-(2-Methoxyphenyl)piperazine, *N*-(4-bromobutyl)phthalimide, hydrazine hydrate, *tert*-butylbromoacetate, potassium carbonate, 1,4,7,10-tetraazacyclododecane (cyclen), trifluoroacetic acid, chloroacetyl chloride, sodium bicarbonate, serotonin hydrochloride, WAY-100635 maleate were purchased from Sigma-Aldrich. Acetonitrile (HPLC grade), *N*,*N*-dimethylformamide (HPLC grade), dichloromethane (HPLC grade), water (HPLC grade), MTT and trifluoroacetic acid were obtained from E. Merck Ltd., India. Metal salts ($GaCl_3$, $EuCl_3$ and $GdCl_3$), DMEM F12, EDTA, nystatin, formaldehyde, D-glucose, agarose and sodium chloride were purchased from Aldrich (99.9%). Penicillin, streptomycin sulfate, FBS and trypsin were purchased from GIBCO (Invitrogen). The reactions demanding anhydrous conditions or involving moisture sensitive reactants were carried out under an atmosphere of dry nitrogen using oven dried (80 °C) glassware. All reaction temperatures reported indicate the temperature of the bath in contact with the reaction vessel. Sep-Pak tC18 Plus short cartridges were purchased from Waters. TLC was run on the silica gel coated aluminum sheets (silica gel 60 F254, Merck, Germany). Instant thin layer chromatography was used to detect radiocomplexation and radiochemical purity. Radio TLC was analyzed on Peak Simple 3.29. Gallium-68 complex radio HPLC was performed on semi automated GE FXFN TracerLab integrated with radioactivity detection and UV detection at 254 nm (fixed wavelength detector K-2001, Knauer, Germany), using isocratic pump SykamS-1021, elution with methanol and water (25/80, v/v) mobile phase and flow rate of 2 mL min^{-1} on C-18 reversed phase Nucleosil column (250 mm × 10 mm, 5 μm). ^1H and ^{13}C NMR spectra were recorded on a Bruker Avance II 400 MHz system (Ultra shield). Chemical shifts 'δ' were reported in ppm relative to TMS. Mass spectra (ESI-MS in positive and negative ion mode) were performed on an in-house Agilent 6310 system ion trap. High resolution mass spectroscopy was done using accurate-mass Quadrupole time-of-flight (Q-TOF) LC/MS at Delhi University. All the computational studies were performed with Schrödinger, LLC, New York, NY, 2014 maestro 9.7.[28] MR studies were done using an inhouse 7 T Bruker Biospec USR 70/30, (AVANCE III) horizontal bore animal MRI scanner tuned to 20 MHz. *In vivo* imaging studies were performed using micro PET imaging as non-invasive technology. The acquisitions were

performed using a GE FLEX Triumph (TriFoil Imaging) micro-PET/SPECT/CT scanner. This scanner consists of a micro-PET module (LabPET4) with 2′2′10 mm^3 LYSO/LGSO scintillators in an 8-pixel, quad-APD detector module arrangement. Potentiometric measurements were carried out with an automatic titration system consisting of metrohm 713 pH meter equipped with Metrohm A.60262.100 electrode, 800 Dosino autoburet. The image processing was done using PMOD 3.2 and Amide 1.0.4 software.

Cell culture

Monolayer cultures of normal embryonic kidney cells, HEK, in DMEM (Sigma, USA) supplemented with 10% fetal bovine serum (GIBCO), 50 U mL^{-1} penicillin, 50 μg mL^{-1} streptomycin sulfate, and 2 μg mL^{-1} nystatin were maintained at 37 °C in a humidified CO_2 incubator (5% CO_2, 95% air). Cells were routinely subcultured using 0.05% trypsin (Sigma, USA) in 0.02% EDTA in humidified atmosphere of 95% air and 5% CO_2 at 37 °C twice a week.

Ethics statement

The human serum study was approved by the institutional ethical committee. Blood samples for human serum study were collected from healthy volunteers who were well informed about the study. Written consent from the volunteers above 18 years of age was obtained.

Animal models

All animal experiments were conducted in accordance with the guidelines of INMAS animal ethics committee (CPCSEA Regn no. 8/GO/a/99). Blood clearance, imaging, and biodistribution were carried on SD rats. Rats were housed under conditions of controlled temperature of 22 ± 2 °C and normal diet *ad libitum*.

Data analysis

The competition curve of the receptor binding experiments was analyzed by nonlinear regression using algorithms in GraphPad PRISM 5.0 (San Diego, CA). Biodistribution data is reported as mean ± standard deviation (S.D.). VOI analyses were carried out on PMOD 3.2.

Synthetic approach

Synthesis of compounds 2-(4-(4-(2-methoxyphenyl)piperazin-1-yl)butyl)isoindoline-1,3-dione (**1**) and 4-(4-(2-methoxyphenyl) piperazin-1-yl)butan-1-amine (**2**) have been done as reported previously by our group.[18]

Synthesis of 2-chloro-*N*-(4-(4-(2-methoxyphenyl)piperazin-1-yl) butyl)acetamide (3)

2-Chloroacetylchloride (410 mg, 3.636 mmol in 10 mL of chloroform) and potassium carbonate (627 mg, 4.5 mmol in 10 mL of water) were added simultaneously through dropping funnels to a stirred solution of **2** (800 mg, 3.03 mmol) in 10 mL of chloroform at 0 °C over a period of 1 h. The reaction mixture was stirred for an additional 4 h at room temperature. The chloroform layer was separated and washed with water (50 mL) twice. The organic layer was dried over anhydrous sodium sulfate and evaporated to product **3** (820 mg, 80%). The product was used as such without any further purification. ^{1}H NMR (400 MHz, 25 °C, $CDCl_3$), δ (ppm): 1.5 (s, 4H, CH_2), 2.3 (s, 2H, CH_2), 2.5 (s, 4H, CH_2), 3.1 (s, 4H, CH_2), 3.3 (t, 2H, $J = 6$ Hz, CH_2), 3.8 (s, 3H, CH_3), 4.0 (s, 2H, CH_2), 6.7–6.9 (m, 4H, CH); ^{13}C NMR (100 MHz, 25 °C, $CDCl_3$), δ (ppm): 24.2, 27.3, 39.7, 42.7, 50.6, 53.5, 55.3, 58.3, 111.1, 118.2, 120.9, 122.9, 141.2, 152.2, 165.8; MS (ESI^+) *m*/*z* calculated for $C_{17}H_{26}ClN_3O_6$ 339.8, found $[M + H]^+$ 340.5.

Synthesis of 1,4,7-tri(*tert*-butoxymethane)-1,4,7,10-tetraazacyclododecane (*t*-Bu-DO3A) (4)

Under an atmosphere of nitrogen, 1,4,7,10-tetraazacyclododecane (2.906 mmol, 500 mg) was dissolved in dry acetonitrile (10 mL) at 0 °C. To the reaction flask $NaHCO_3$ (8.72 mmol, 732 mg) was added and stirred for 30 min. *tert*-Butyl bromoacetate (8.72 mmol, 1.28 mL) was added slowly from a dropping funnel in 2 h at 0 °C. The reaction was stirred for additional 1 h at 0 °C and then at room temperature for 40 h. The progress of the reaction was checked by TLC (9 : 1; dichloromethane : methanol). After the completion of the reaction, the reaction mixture was filtered and the filtrate was evaporated to dryness. The crude compound was purified by column chromatography (silica gel, 10% methanol in dichloromethane, R_f 0.67) to give final compound *t*-Bu-DO3A (1120 mg, 75%) as white powder. ^{1}H NMR (400 MHz, 25 °C, $CDCl_3$); 1.4 (27H, s, $C(CH_3)_3$), 2.8–3.1 (16H, m, CH_2), 3.2–3.3 (6H, m, CH_2); ^{13}C NMR (400 MHz, 25 °C, $CDCl_3$): 28.0, 47.5, 49.1, 51.1, 55.6, 58.2, 81.7, 170.5, 172.9; *m*/*z* calculated for $C_{26}H_{50}N_4O_6$ 514.7, found 515.8 $[M + H]^+$.

Synthesis of *tert*-butyl 2,2′,2″-(10-(2-(4-(4-(2-methoxyphenyl) piperazin-1-yl)butylamino)-2-oxoethyl)-1,4,7,10-tetraazacyclododecane-1,4,7-triyl)triacetate (5)

Under nitrogen atmosphere, to a stirring solution of 1,4,7-tris(carbobutoxymethyl)-1,4,7,10-tetraaza-cyclododecane (500 mg, 0.97 mmol) in dry acetonitrile (20 mL), K_2CO_3 (669 mg, 4.85 mmol) was added. After 30 min, (**3**) (396 mg, 1.17 mmol) dissolved in acetonitrile was added drop wise and heated to 70 °C. After 24 h, the reaction mixture was cooled to room temperature, filtered, and evaporated under reduced pressure to give crude oily residue. The compound was purified by column chromatography (silica gel, 5% methanol in dichloromethane) to give the ligand (**5**) as a brown solid (600 mg, 75%). ^{1}H NMR (400 MHz, 25 °C, $CDCl_3$), δ (ppm): 1.4 (s, 27H, $C(CH_3)_3$), 1.6–3.3 (m, 40H, CH_2), 3.8 (s, 3H, CH_3), 6.8–6.9 (m, 4H, CH), 8.4 (br, 1H, NH); ^{13}C NMR (100 MHz, 25 °C, $CDCl_3$), δ (ppm): 22.9, 26.6, 27.9, 38.5, 49.2, 52.8, 55.7, 56.1, 57.6, 81.8, 111.2, 118.4, 120.9, 133.2, 140.5, 152.2, 171.5, 172.3. HRMS (ESI^+) *m*/*z* calculated for $C_{43}H_{75}N_7O_8$ 817.5677, found $[M + H]^+$ 818.5756, $[M + Na]^+$ 840.5572 (see ESI† Fig. S9).

Synthesis of 2,2′,2″-(10-(2-(4-(4-(2-methoxyphenyl)piperazin-1yl)butylamino)-2-oxoethyl)-1,4,7,10-tetraazacyclododecane-1,4,7-triyl)triacetic acid (6)

The ligand **5** (500 mg, 0.595 mmol) was dissolved in dichloromethane (4 mL) and 1 mL of trifluoroacetic acid was added at

0 °C and stirred for 4 h. The reaction mixture was stirred at room temperature for additional 10 h. The solvent was evaporated and residue was dissolved in 1 mL of methanol, followed by addition of 30 mL of diethyl ether drop wise at 0–5 °C and stirring for 1 h at room temperature. The solvent was decanted and the precipitated compound dried under reduced pressure. (370 mg, 96%). ^{1}H NMR (400 MHz, 25 °C, D_2O), δ (ppm): 1.4 (m, 2H, CH_2), 1.6 (m, 2H, CH_2), 2.6–3.9 (m, 39H, CH_2 and CH_3 of $-OCH_3$), 6.8–6.9 (m, 2H, CH), 7.0–7.1 (m, 2H, CH); ^{13}C NMR (100 MHz, 25 °C, $CDCl_3$), δ (ppm): 13.9, 20.6, 25.3, 38.3, 48.1, 48.7, 50.1, 53.8, 54.1, 55.2, 56.2, 65.9, 111.9, 114.8, 116.2, 117.7, 120.6, 121.2, 126.7, 135.9, 151.8, 162.3, 163.4, 171.5 HRMS (ESI^+) m/z calculated for $C_{31}H_{51}N_7O_8$ 649.3799, found $[M + H]^+$ 650.3999 (see ESI† Fig. S11).

Complexation of DO3A-butyl-MPP with $EuCl_3$

To a solution of DO3A-butyl-MPP (200 mg; 0.3076 mmol) in water (10 mL) was added $EuCl_3 \cdot 6H_2O$ (112.5 mg; 0.3076 mmol) and the pH of the reaction mixture was adjusted to 5.5. The reaction was stirred at 60 °C for 6 h. The reaction mixture was filtered and the solvent was evaporated to obtain the Eu-complex as a pale green solid. HR-ESI-MS calculated for $C_{31}H_{48}EuN_7O_8$ 800.2855, found $[M + H]^+$ 800.2840.

Complexation of DO3A-butyl-MPP with $GdCl_3$

To a solution of DO3A-butyl-MPP (200 mg; 0.3076 mmol) in water (10 mL) was added $GdCl_3 \cdot 6H_2O$ (114 mg; 0.3076 mmol) and the pH of the reaction mixture was adjusted to 5.5. The reaction was stirred at 60 °C for 12 h. The reaction mixture was filtered and the solvent was evaporated to obtain the Gd complex as a pale white solid. HR-ESI-MS $C_{31}H_{48}GdN_7O_8$ calculated for 804.2805, found $[M + H]^+$ 805.2896.

Complexation of DO3A-butyl-MPP with $GaCl_3$

10 mg (0.0153 mmol) DO3A-butyl-MPP was dissolved in water and pH was adjusted to 4.5 with the help of 1 M sodium acetate solution. The resulting solution was perched with nitrogen to maintain inert atmosphere. Then $GaCl_3$ (3.2 mg) was added. The temperature of reaction mixture was then raised to 80 °C for 8 h. After that the solution was brought to room temperature and chelex 100 was added to it which was then stirred for 30 min. Then the solution was filtered and evaporated under reduced pressure to give a white colored compound. HRMS (ESI^+) calculated for $C_{31}H_{48}GaN_7O_8$: 715.2820, found $[M]^+$ 713.0644.

Relaxation measurements

MR imaging was done using an inhouse 7 T Bruker Biospec USR 70/30, (AVANCE III) horizontal bore animal MRI scanner. For all experiments, RARE T_1 + T_2 sequence was used to acquire relaxometry images. The scan was acquired at 5 TE times (11, 33, 55, 77, 99 ms) and at different TR's (6000, 5000, 4500, 4000, 3500, 3000, 2500 and 1981 ms). Relaxation data were analyzed with Topspin 2.0 (Bruker) software.

Spectroscopic measurement

The luminescence lifetime was obtained by measuring the decay at the maximum of emission spectra and the signals were analyzed as single exponential decays. The instrument settings were: gate-time of 10 ms, integration time of 1 s, flash count – 8 and proper slit widths were used. The excitation wavelength used for Eu-DO3A-butyl-MPP was 365 nm and luminescence lifetimes are the average of five independent experiments. The slit widths for both excitation and emission monochromators were kept open. The number of coordinated water molecules (q) present in the inner sphere of the complex is calculated by using equation of Supkowski and Horricks for Eu(III).

$$q = A_{Eu}(1/\tau_{H_2O} - 1/\tau_{D_2O} - a_{Eu})$$

Solutions of Eu(III) complexed DO3A-butyl-MPP complex were prepared by mixing its appropriate volume in MilliQ water or in D_2O and ligand in Tris buffer 0.1 M (pH = 7.4) or in D_2O followed by addition of NaOD until pH = 7. Measurement of the Ln(III) luminescence lifetimes in solutions of H_2O and D_2O gave the estimation of the number of coordinated water molecules present in complex by using above equation.

Potentiometric titrations

Potentiometric titrations were carried out at 25 °C and ionic strength "I" = 1 M *tert*-butylammoniumchloride (TBACl). The protonation constant of DO3A-butyl-MPP were determined potentiometrically by titrating 2 mM of HCl (2 mL) in the presence of 0.1 mM DO3A-butyl-MPP (15 mL) with 0.01 mM (3 mL) *tert*-butylammoniumhydroxide (TBAOH). Titrations were performed in the pH range of 1.0–10.0 for protonation constants. The protonation constant of ligand is expressed by eqn (1) and stability constant of the metal complex is given by eqn.

$$K_i = \frac{[H_iL]}{[H_{i-1}L][H^+]} \quad (1)$$

$$K_{MH_iL} = \frac{[MH_iL]}{[MH_{i-1}L][H^+]} \quad \text{where } i = 0,\ 1,\ 2,\ 3 \quad (2)$$

Radiolabeling of DO3A-butyl-MPP with ^{68}Ga

^{68}Ga was eluted from ^{68}Ge/^{68}Ga generator (Eckert and Ziegler) with 0.1 N HCl (3 mL) to obtain 480 MBq of ^{68}Ga. Sodium acetate was added to adjust pH of the elute 4. Then compound (200 μg) was added from 1 mg mL^{-1} stock solution of the compound and the mixture incubated at 90 °C for 10 min. It was then cooled and passed through C-18 cartridge (preconditioned with ethanol and water). The compound was eluted with 1 mL ethanol. Then ITLC was run in 0.15 M sodium acetate. The radiochemical purity was assessed by omniscan EZ-TLC scanner and then the radiolabeled conjugate was purified using a C-18 reversed phase extraction cartridge which was preconditioned with 20 mL methanol and subsequently activated with 30%

methanol. The cartridge was successively rinsed with 5 mL distilled water and radiolabeled conjugate was eluted in 5 mL of 40% ethanol. The ^{68}Ga-DO3A-butyl-MPP was reconstituted in saline, and filtered through a sterile 0.22 μm Millipore (Milford, MA) Millex-GV® disposable syringe filter. Radiotracer purity and stability were monitored using radio-HPLC. In each HPLC analysis, the eluent was collected and counted along with a standard prepared from the injectate.

Determination of log *P* and stability in blood serum. The partition coefficient of the complex was determined by measuring the activity that partitioned between the 1-octanol and aqueous phosphate buffer (0.025 mol L^{-1}, pH 7.4) under strict equilibrium conditions. 2 mL 1-octanol and 2 mL of ^{68}Ga-DO3A-butyl-MPP phosphate buffer were mixed in a centrifuge tube. The mixture was vortexed at room temperature for 5 min and then centrifuged at 5000 rpm min^{-1} for 5 min. The counts in 0.1 mL samples of both organic and inorganic layers were determined by a well type gamma counter. The measurement was repeated three times. The partition coefficient (P) was calculated as a ratio of the counts in the octanol fraction to the counts in the water fraction (average of $n = 5$).

Human serum stability. Fresh human serum was prepared by allowing blood collected from healthy volunteers to clot for 1 h at 37 °C in a humidified incubator maintained at 5% carbon dioxide/95% air. Then, the samples were centrifuged at 400*g*, and the serum was filtered through 0.22 μm syringe filter into sterile tubes. The radiolabeled DO3A-butyl-MPP was immediately placed in a CO_2 chamber incubated at 37 °C and then analyzed to check for any dissociation of the complex. The mixture was stored in the same environment conditions, and aliquots of 100 mL (in triplicate) were taken at appropriate periods of time (0 min, 30 min, 1 h and 3 h). The aliquots were treated with 200 μL of ethanol, cooled (4 °C), and centrifuged during 15 min at 4000 rpm, at 4 °C, in order to precipitate the serum proteins. A 200 μL aliquot of supernatant was collected for activity counting in a γ well-counter. The sediment was washed twice with 1 mL of ethanol and its activity was counted. The activity of the supernatant was compared to that of the sediment in order to determine the percentage of the chelate associated to the proteins. The activity of the supernatant at 3 h was evaluated by TLC in order to check whether the chelate remained intact.

Biological studies

Cell viability assay of DO3A-butyl-MPP. To test the cytotoxic effect of DO3A-butyl-MPP exposure on cells, MTT assays were conducted. Exponentially growing cells were plated in a 96 well microtitre plate at a cell density of 4000 cells per well for 24 h before treatment. Cells were treated with the varying concentrations of the drug (0.001–10 mM) at different time intervals 24 h, 48 h, 72 h. At the end of treatment, both the treated cells and negative control were incubated with MTT at a final concentration of 0.05 mg mL^{-1} for 2 h at 37 °C and followed by removal of the medium. Triplicate wells from each treatment were lysed and the formazan crystals were dissolved using 150 μL of DMSO. Optical density of 150 μL of extracts at 570 nm was measured (reference filter: 630 nm). Surviving fraction at (0.001–10 mM) concentration range was plotted against concentration for DO3A-butyl-MPP.

Measurement of ^{68}Ga-DO3A-butyl-MPP uptake in hippocampal primary cultures. Primary cultured cortical neuronal cells were obtained from the hippocampus of fetal SD rats at 17–20 days of gestation. Single cell suspension from the hippocampus of fetal rats was seeded on the poly-L-lysine coated culture slide at 3×10^5 cells per well. Culture was incubated in DMEM (F-12) medium supplemented with 10% heat inactivated horse serum and 5% fetal bovine serum for 1–7 days after plating together with glutamine 2.5 mM, glucose 17.5 mM, and $NaHCO_3$ 14.3 mM. The cultures were maintained at 37 °C in a humidified 5% CO_2 atmosphere. After 3 days non-neuronal cells were removed by addition of cytosine arabinoside (10 μM). Only mature cultures surviving 15–18 days *in vitro* were used for the experiments. After 18 days of culture *in vitro*, successful cultured neurons were selected for binding studies which were carried out as described previously.[20] The amount of radioactivity (CPM) in cell lysates was determined by gamma scintillation counting. Uptake was then calculated and expressed in units of pmoles per μg protein per min. Competitive binding of ^{68}Ga-DO3A-butyl-MPP with unlabeled serotonin and WAY-100635 were assessed to calculate dissociation constant (K_d). Final concentrations in the well were 10 pM to 10 μM. Hippocampal cultures were washed with HBSS and were incubated in HBSS at 37 °C for 20 min prior to the experiment. Binding experiments were performed at 37 °C. Cells were incubated for 30 min with increasing concentrations (10 pM to 10 μM) of ^{68}Ga-DO3A-butyl-MPP in the absence and presence of the 100 folds excess unlabeled serotonin/WAY100635 to estimate the total binding and non-specific binding respectively. Specific binding was obtained by subtracting non-specific binding from total binding. The cells were washed with cold PBS and 0.9% saline four times at the end of each experiment. Gamma scintillation counting was used to determine the cell-associated radioactivity.

5-HT$_{1A}$ receptor binding assay. The hippocampus of rat brain was homogenized in 10 volumes of ice-cold buffer (50 mM Tris–HCl pH-7.6) using an Ultra Turrax T10 (IKA). The homogenate was centrifuged for 10 min at 20 000*g*. The resulting pellet was resuspended with the Ultra-Turrax and centrifuged again at 20 000*g* for 10 min. The same procedure was repeated again. After that the pellet was resuspended in 10 volumes of buffer and stored at −80 °C until used in binding studies.

The binding assay was carried out in a final volume of 2.5 mL Tris–HCl buffer (50 mM, pH 7.4, 0.1% ascorbic acid, 2 mM $CaCl_2$) containing varied concentrations (1 nM to 1 μM) of the ^{68}Ga-DO3A-butyl-MPP complex and membrane homogenate (about 0.5 mg per mL protein). Nonspecific binding was determined as the amount of ^{68}Ga-DO3A-butyl-MPP bound in the presence of 10 mM serotonin. The binding assay was conducted in triplicates at 20 °C for 120 min. The incubation was terminated by rapid filtration through GF/B glass fiber filters. The filters were rapidly washed with 4 mL portions of ice cold buffer, transferred into 4 mL scintillation cocktail and analyzed for radioactivity by scintillation counting.

5-HT$_{2A}$ receptor binding assay. The cortex of rat brain was homogenized and prepared analogously to the procedure described above and stored at −80 °C until used in binding studies. The assay was performed in a volume of 5.0 mL Tris–HCl buffer (pH 7.6) containing 100 folds excess of ketanserin tartarate, membrane homogenate (about 0.9 mg per mL protein) and various concentrations (1 nM to 1 μM) of ^{68}Ga-DO3A-butyl-MPP. Triplicates of the samples were incubated at 20 °C for 60 min. Filtration and counting of the samples were the same as described above.

5-HT transporter binding assay. The caudate nucleus of rat brain was homogenized and prepared analogously to the procedure described above and stored at −80 °C until used in binding studies. The final volume of the binding assay was 5.0 Tris–HCl buffer (pH 7.4) containing 120 mM NaCl, 5 mM KCl, membrane homogenate (about 1.2 mg per mL protein) and various concentrations (1 nM to 1 μM) of the ^{68}Ga-DO3A-butyl-MPP complex in presence and absence of 100 fold excess of paroxetine. Filtration and counting of the samples were the same as described above.

PET acquisition. Animals were anesthetized by inhalation of 2% isoflurane in 2 L min^{-1} oxygen in the prone position. Animals were injected with 37 MBq activity of ^{68}Ga-DO3A-butyl-MPPimmediately prior to their micro PET scan on the camera bed at the start of a dynamic acquisition. Frames of 1 × 1 and 5 × 5 min were accordingly sequentially recorded for 60 min. The resulting PET was reconstructed using 50 iterations of the maximum likelihood expectation maximization algorithm.

***In vivo* MR imaging.** The animals were anaesthetized and injected with the Gd-DO3A-butyl-MPP at 2 mM concentration through tail vein. MR images were acquired using loop coil on brain. T_1 measurements were performed using a fast spin echo sequence with TRs from 140–6000 ms with TE = 8 ms. The slice thickness, matrix and pixel size were same for all treated and control animals.

Plasma clearance and biodistribution. Plasma clearance is a quantitative study and reveals about the clearance kinetics of the drug. Radiolabeled conjugate ^{68}Ga-DO3A-butyl-MPP 200 μL (10 μmol kg^{-1}, 14.8 MBq activity) was administered intravenously through the tail vein of the SD rats (n = 3). Blood samples were withdrawn at different time intervals (0, 5, 10, 15, 20, 30, 60, 120 and 240 min). Decay corrected radioactivity is expressed as % injected dose assuming theoretical blood volume to be approximately 7% of the body weight. Plasma clearance was plotted as μg mL^{-1} min^{-1} against time.

For biodistribution, twelve SD rats (weighing 110–140 g) were divided into 4 groups (n = 3) for time intervals-10 min, 30 min, 1 h and 4 h. Intravenous injection of ^{68}Ga-DO3A-butyl-MPP conjugate in a volume of 100 μL (5 μmol kg^{-1}, 8.14 MBq activity) was injected through the tail vein of each rat. Rats were dissected at 10 min, 30 min, 1 h and 4 h post injection. Various organs were removed, made free of adhering tissue, rinsed with chilled saline, blotted to remove excess liquid, weighed, and radioactivity measured in each organ in a gamma counter calibrated for ^{68}Ga energy. Uptake of the radiotracer in each tissue was evaluated and expressed as percentage injected dose per gram of the tissue (% ID per g). Animal protocols have been approved by Institutional Animal Ethics Committee and in accordance with the guidelines of INMAS animal ethics committee (CPCSEA Regn no. 8/GO/a/99).

Brain biodistribution experiment. Three adult SD rats weighing between 300 and 350 g were used in the procedure. Intravenous injection of 0.5 mL of labeled ^{68}Ga-DO3A-butyl-MPP solution in 5% ethanol with an activity of 6.1 MBq was injected through the tail vein to each rat. After 10, 30 and 45 min, the rats were dissected and the brains were removed and placed in ice, washed with physiological saline, their weight measured on an analytical balance and their activity counted. The brains were then dissected, and the weights of the following regions were calculated: hippocampus, caudate putamen, cortex and cerebellum. The radioactivity in each section was counted and regional uptake of the ligand was assessed.

Computational methodology

The homology model for human 5-HT$_{1A}$ receptor was prepared as per our previously reported study[24] by using prime homology modeling.[25] The 5-HT$_{1A}$ model was built on crystal structure of the β_2-adrenergic receptor as template. The model was refined by using protein preparation wizard of Schrödinger[28] and optimized for further docking studies. Also, the ligand, 'DO3A-butyl-MPP' was prepared using the Ligprep v2.9 module.[23] All the possible protonation states at pH = 7.0 ± 2.0 were generated using ionization tool. Specified chiralities of these ligands were retained during ligand preparation. Low energy conformers were obtained in the force field OPLS2005 without any constraints. These conformers were retained for docking studies. We have performed docking studies of all structured 5-HT$_{1A}$ models on the known binding sites and corresponding grids were generated. Flexible (IFD) docking studies were performed to predict the binding mode of the ligand with high accuracy where the Glide docking under extra precision (XP) mode was employed. Post docking minimizations were performed by including five poses per ligand.

Acknowledgements

We are thankful to Dr R. P. Tripathi, Director of Institute of Nuclear Medicine and Allied Sciences, Defence Research and Development Organization and Department of Chemistry, University of Delhi for providing excellent research facilities. We are also thankful Dr Poonam Rana for MR imaging at NMR Research Centre, INMAS. This work was supported by INMAS Project INM-311(3.1).

Notes and references

1 J. Passchier and A. V. Waarde, *Eur. J. Nucl. Med.*, 2001, **28**, 113.

2 (*a*) N. Aznavour and L. Zimmer, *Neuropharmacology*, 2007, **52**, 695; (*b*) C. Gross, X. Zhuang, K. Stark, S. Ramboz, R. Oosting, L. Kirby, L. Santarelli, S. Beck and R. Hen, *Nature*, 2002, **416**, 396.

3 (*a*) W. C. Drevets, E. Frank, J. C. Price, D. J. Kupfer, P. J. Greer and C. Mathis, *Nucl. Med. Biol.*, 2000, **27**, 499; (*b*) F. Fiorino, B. Severino, E. Magli, A. Ciano, G. Caliendo, V. Santagada, F. Frecentese and E. Perissutti, *J. Med. Chem.*, 2014, **57**, 4407.

4 (*a*) L. Rodriguez, M. L. Ayala, D. Benhamu and M. J. Morcillo, *Curr. Med. Chem.*, 2002, **9**, 443; (*b*) H. Pessoa-Mahana, R. Araya-Maturana, B. C. Saitz and C. D. Pessoa-Mahana, *Mini-Rev. Med. Chem.*, 2003, **3**, 77; (*c*) P. Zajdel, G. Subra, A. J. Bojarski, B. Duszynska, M. Pawlowski and J. Martinez, *Bioorg. Med. Chem. Lett.*, 2006, **16**, 3406; (*d*) J. L. Wang, E. C. Deutsch, S. Oya and H. F. Kung, *Nucl. Med. Biol.*, 2010, **37**, 577; (*e*) J. P. Holland, M. W. Jones, P. D. Bonnitcha, J. S. Lewis and J. R. Dilworth, *New J. Chem.*, 2009, **33**, 1845; (*f*) S. Houle, J. N. DaSilva and A. A. Wilson, *Nucl. Med. Biol.*, 2000, **27**, 463; (*g*) R. A. Hussainy, J. Verbeek, D. V. D. Born, J. Booij and J. D. M. Herscheid, *Eur. J. Med. Chem.*, 2011, **46**, 5728; (*h*) R. K. Raghupati, L. Rydelek-Fitzgerald, M. Teitler and R. A. Glennon, *J. Med. Chem.*, 1991, **34**, 2633.

5 (*a*) A. A. Wilson, J. N. Dasilva and S. Houle, *Nucl. Med. Biol.*, 1996, **23**, 487; (*b*) S. Marchais, B. Nowicki, H. Wikstrom, L. T. Brennum, C. Halldin and V. W. Pike, *Bioorg. Med. Chem.*, 2001, **9**, 695.

6 (*a*) D. L. Bars, C. Lemaire, N. Ginovart, A. Plenevaux, J. Aerts, C. Brihaye, W. Hassoun, V. Leviel, P. Mekhsian, D. Weissmann, J. F. Pujol, A. Luxen and D. Comar, *Nucl. Med. Biol.*, 1998, **25**, 343; (*b*) L. Lang, E. Jagoda, B. Schmall, M. Sassaman, Y. Ma and W. C. Eckelman, *Nucl. Med. Biol.*, 2000, **27**, 457.

7 F. Rosch and R. P. Baum, *Dalton Trans.*, 2011, **40**, 6104.

8 L. Lattauda, A. Barge, G. Cravotto, G. B. Giovenzana and L. Tei, *Chem. Soc. Rev.*, 2011, **40**, 3019.

9 K. Tanaka and K. Fukase, *Org. Biomol. Chem.*, 2008, **6**, 815.

10 S. Liu, *Adv. Drug Delivery Rev.*, 2008, **60**, 1347–1370.

11 (*a*) C. J. Anderson and M. J. Welch, *Chem. Rev.*, 1999, **99**, 2219; (*b*) M. J. Welch, C. S. Redvanly and N. J. Hoboken, *Handbook of radiopharmaceuticals, radiochemistry and applications*, Wiley, Chichester England, 2003, p. 848.

12 L. E. Jennings and N. J. Long, *Chem. Commun.*, 2009, 3511.

13 M. Suchy, R. Bartha and R. H. E. Hudson, *RSC Adv.*, 2013, **3**, 3249.

14 R. A. Glennon, *Drug Dev. Res.*, 1992, **26**, 251.

15 J. L. Mokrosz, M. J. Mokrosz, S. Charackchieva-Minol, M. H. Paluchwaska, A. J. Bojarski and B. Duszyriska, *Arch. Pharm.*, 1995, **328**, 143.

16 A. Orjales, L. Alonso-Cires, L. Labeaga and R. Corcostegui, *J. Med. Chem.*, 1995, **38**, 1273.

17 M. L. Lopez-Rodriguez, M. J. Morcillo, E. Fernandez, M. L. Rosado, L. Pardo and K. J. Schaper, *J. Med. Chem.*, 2001, **44**, 198.

18 N. Singh, P. P. Hazari, S. Prakash, K. Chuttani, H. Khurana, H. Chandra and A. K. Mishra, *MedChemComm*, 2012, **3**, 814.

19 A. E. Merbach and E. Toth, *The Chemistry of Contrast Agents in Medical Magnetic Resonance Imaging*, Wiley, England, 2001.

20 A. K. Pandey, P. P. Hazari, R. Patnaik and A. K. Mishra, *Brain Res.*, 2011, **1383**, 289.

21 M. Nishi and E. C. Azmitia, *Brain Res.*, 1996, **722**, 190.

22 K. P. Zuideveld, N. Treijtel, H. J. Maas, J. M. Gubbens-stibbe, L. A. Peletier, P. H. Van der graaf and M. Danhof, *J. Pharmacol. Exp. Ther.*, 2001, **300**, 330.

23 (*a*) Y. D. Paila, S. Tiwari, D. Sengupta and A. Chattopadhyay, *Mol. BioSyst.*, 2011, **7**, 224; (*b*) F. M. McRobb, B. Capuano, I. T. Crosby, D. K. Chalmers and E. Yuriev, *J. Chem. Inf. Model.*, 2010, **50**, 626.

24 P. P. Hazari, J. Schulz, D. Vimont, N. Chadha, M. Allard, M. Szlosek-Pinaud, E. Fouquet and A. K. Mishra, *ChemMedChem*, 2013, **9**, 337.

25 O. M. Becker, Y. Marantz, S. Shacham, B. Inbal, A. Heifetz, O. Kalid, S. Bar-Haim, D. Warshaviak, M. Fichman and S. Noiman, *Proc. Natl. Acad. Sci. U. S. A.*, 2004, **101**, 11304.

26 B. Y. Ho, A. Karschin, T. Branchek, N. Davidson and H. A. Lester, *FEBS Lett.*, 1992, **312**, 259.

27 I. Heimbold, A. Drews, M. Kretzschmar, K. Varnas, H. Hall, C. Halldin, R. Syhre, W. Kraus, H.-J. Pietzsch, S. Seifert, P. Brust and B. Johannsen, *Nucl. Med. Biol.*, 2002, **29**, 375.

28 *Protein prepwizard, Ligprep version 3.0, Glide version 6.2*, Schrödinger, LLC, New York, NY, 2014.